Original Article

LncRNA *HOXD-AS2* regulates *miR-3681-5p/DCP1A* axis to promote the progression of non-small cell lung cancer

Yuanyuan Zhang[1,2], Haitao Ma[1,3]

[1]Department of Thoracic Surgery, The First Affiliated Hospital of Soochow University, Suzhou, China; [2]Department of Thoracic Surgery, Binhai County People's hospital, Yancheng, China; [3]Department of Thoracic Surgery, Dushu Lake Hospital Affiliated to Soochow University, Suzhou, China

Contributions: (I) Conception and design: Y Zhang; (II) Administrative support: H Ma; (III) Provision of study materials or patients: Both authors; (IV) Collection and assembly of data: Y Zhang; (V) Data analysis and interpretation: Y Zhang; (VI) Manuscript writing: Both authors; (VII) Final approval of manuscript: Both authors.

Correspondence to: Haitao Ma. Department of Thoracic Surgery, Dushu Lake Hospital Affiliated to Soochow University, Suzhou 215000, China; Department of Thoracic Surgery, The First Affiliated Hospital of Soochow University, Suzhou 215000, China. Email: mht7403@163.com.

Background: Non-small cell lung cancer (NSCLC) is the most common malignancy in lung cancer, with a low survival rate and unfavorable prognosis. Dysregulated long non-coding RNAs (lncRNAs) play vital functions in tumor progression. This study intended to probe the expression pattern and function of *HOXD-AS2* in NSCLC.

Methods: Quantitative real-time polymerase chain reaction (qRT-PCR) was conducted to analyze the expression of *HOXD-AS2*, *miR-3681-5p*, *CCR1*, mRNA-decapping enzyme 1A (*DCP1A*), and *PPP3R1*. Cell viability, migration, and invasion were separately examined via 3-(4,5-dimethylthiazolyl-2)-2,5-diphenyltetrazolium bromide (MTT) and transwell experiments. Luciferase reporter assay was conducted to evaluate the binding of *miR-3681-5p* with *HOXD-AS2* or *DCP1A*. Protein expression of *DCP1A* was assessed via Western blot. NSCLC animal models were constructed through injection of H1975 cells transfected with lentivirus (LV)-sh-HOXD-AS2 into nude mice, followed by hematoxylin and eosin (HE) staining and immunohistochemistry (IHC) analysis.

Results: In this study, *HOXD-AS2* was upregulated in NSCLC tissues and cells, and high *HOXD-AS2* predicted short overall survival (OS). Downregulation of *HOXD-AS2* could impair the proliferation, migration, and invasion abilities of H1975 and A549 cells. *MiR-3681-5p* was shown to bind with *HOXD-AS2* and be lowly expressed in NSCLC. Suppression of *miR-3681-5p* could abolish the inhibitory effect of *HOXD-AS2* silencing on proliferation, migration, and invasion. *DCP1A* was screened as the target of *miR-3681-5p* and its overexpression could rescue *miR-3681-5p* upregulation-repressed proliferation, migration, and invasion activities. Moreover, animal experiments affirmed that *HOXD-AS2* promoted tumor growth *in vivo*.

Conclusions: *HOXD-AS2* modulates the *miR-3681-5p/DCP1A* axis to boost the progression of NSCLC, which founds the basis of *HOXD-AS2* as a new diagnostic biomarker and molecular target for NSCLC therapy.

Keywords: Non-small cell lung cancer (NSCLC); *HOXD-AS2*; *miR-3681-5p*; *DCP1A*

Submitted Dec 26, 2022. Accepted for publication Mar 17, 2023. Published online Mar 27, 2023. This article was updated on December 28, 2023.

The original version was available at: https://dx.doi.org/10.21037/jtd-23-153

doi: 10.21037/jtd-23-153

Introduction

Globally, lung cancer is the most common malignancy and the leading cause of cancer mortality, with a low 5-year survival rate of 6–13% (1,2). It can be divided into small cell lung cancer (SCLC; 15%) and non-small cell lung cancer (NSCLC; 85%), NSCLC can be subdivided into large cell lung cancer, lung adenocarcinoma (LUAD) and lung squamous cell carcinoma (LUSC) (3,4). Surgery, immunotherapy, chemotherapy, radiotherapy, and molecular targeted therapy are main treatment approaches for NSCLC (5). Despite recent advances in treatment strategies of NSCLC, its incidence rate remains relatively high (6). Thus, it is imperative to seek the functional molecular mechanisms in NSCLC to determine new therapeutic targets.

Non-coding RNAs (ncRNAs), constituting the majority of the human transcribed genome, are RNA transcripts that functionally mediate cellular processes, containing transcription, chromatin remodelling, and post-transcriptional modifications (7,8). They can be classified into long ncRNAs (lncRNAs), circular RNAs (circRNAs), microRNAs (miRNAs), small nuclear RNAs (snRNAs), and so on (9). LncRNAs, with a length over 200 nt and no protein-coding potential, are differentially expressed and exert pivotal roles in modulating cellular activities in diverse carcinomas (10-12). For examples, lncRNA *OXCT1-AS1* could boost proliferation of NSCLC cells through targeting *miR-195/CCNE1* axis (13); lncRNA *B4GALT1-AS1* accelerates NSCLC growth via elevating ZEB1 level via sponging *miR-144-3p* (14). Among these lncRNAs, HOXD cluster antisense RNA 2 (*HOXD-AS2*) is a demonstrated oncogenic lncRNA in human carcinomas. In glioma, *HOXD-AS2* is up-regulated and promotes cancer process, which is due to the transcription activation by *TFE3* and cytoplasmic degradation by *miR-661* (15). *HOXD-AS2* also negatively affects the *miR-3681-5p* level to augment *MALT1* expression in glioblastoma (16). Thus, the function and related functional mechanisms underlying *HOXD-AS2* in NSCLC still await investigation.

MiRNAs are small ncRNAs post-transcriptionally controlling gene expression upon targeting 3' untranslated regions (3'UTRs) of relative messenger RNAs (mRNAs) (17). Different to lncRNAs, the length of miRNAs is about 20–22 nt (18). MiRNAs display abnormal expression profiles and functions in human diseases, including cancer (19). *MiR-106b-5p* has been shown to provoke the lung metastasis of breast cancer through targeted inhibition of *CNN1* to activate the *Rho/ROCK1* pathway (20). In prostate cancer, *miR-19a* binds with *CUL5* to hasten migratory, invasive, and epithelial-mesenchymal transition (EMT) capabilities (21). In this research, *miR-3681-5p* is shown to be negatively affected by *HOXD-AS2*, thus augmenting *MALT1* expression for glioblastoma aggressiveness (16). However, no studies on the role of *miR-3681-5p* in NSCLC were conducted.

In the competing endogenous RNA (ceRNA) molecular mechanism, mRNAs commonly function as the downstream targets of miRNAs to influence cellular activities of tumor cells (22,23). Among these genes, mRNA-decapping enzyme 1A (*DCP1A*) is in close association with cancer progression. *DCP1A* is highly expressed and related to poor prognosis, downregulation of which can reduce proliferation, migration, and chemotherapeutic resistance (24). Also, overexpression of *DCP1A* decreases the survival rate of colorectal carcinoma patients (25). In gastric cancer, *DCP1A* is mediated by the *LINC00339/miR-377-3p* axis and accelerates tumor progression (26). Similarly, no studies on the role of *DCP1A* in NSCLC have been reported.

In this paper, we aimed to investigate the role of *HOXD-AS2* in NSCLC in another way. We analyzed the expression of *HOXD-AS2* in cancer tissues and cells and dissected the relationship between its expression and overall survival (OS) of patients. Functional experiments were conducted to examine the effect of *HOXD-AS2* on cell viability, invasion, migration, and apoptosis in NSCLC cells. Thereafter, the binding between *miR-3681-5p* and *HOXD-AS2* or *DCP1A* was explored via luciferase reporter assay. The regulatory function of *HOXD-AS2* on *miR-3681-5p* or that of *miR-3681-5p* on *DCP1A* in NSCLC was measured through rescue experiments. We present the following article

Highlight box

Key findings

- HOXD-AS2 is significantly heightened in NSCLC and it modulates the miR-3681-5p/DCP1A axis to boost the proliferation, migration, and invasion activities of NSCLC cells.

What is known and what is new?

- NSCLC is the most common malignancy in lung cancer, with a low survival rate and unfavorable prognosis. HOXD-AS2 is a demonstrated oncogenic lncRNA in carcinomas.
- The expression profile and molecular mechanism underlying HOXD-AS2 in NSCLC was first uncovered by the present paper.

What is the implication, and what should change now?

- These findings found the basis of HOXD-AS2 as a new diagnostic biomarker and molecular target for NSCLC therapy.

in accordance with the ARRIVE and MDAR reporting checklists (available at https://jtd.amegroups.com/article/view/10.21037/jtd-23-153/rc).

Methods

Clinical tissue samples

We collected 5 paired cancerous and adjacent non-tumor tissues from patients pathologically diagnosed with NSCLC at Binhai County People's Hospital. Tissues were stored at −80 ℃ for subsequent analysis. None of the included patients underwent chemotherapy or radiotherapy prior to tissue collection and all patients provided their informed consents before taking part. The research was approved by the Ethics Committee of Binhai County People's Hospital (No. 2021BYKYLL006) and conducted in accordance with the Declaration of Helsinki (as revised in 2013).

Cell culture

The cells used in assays were obtained from American Type Culture Collection (ATCC; Manassas, VA, USA) and cultivated in a humid environment with 5% CO_2 at 37 ℃. Dulbecco's modified Eagle medium (DMEM; Gibco, Grand Island, NY, USA) supplemented with 100 μg/mL streptomycin, 10% fetal bovine serum (FBS), and 100 U/mL penicillin (Gibco, USA) was employed for culture of human cancerous H1975 (cat. No. CRL-5908), A549 (cat. No. CCL-185), and H1299 (cat. No. CRL-5803) cells, and the normal lung epithelial cell line BEAS-2B (cat. No. CRL-9609) was used as a control.

Quantitative real-time polymerase chain reaction (qRT-PCR)

RNA extraction was implemented in tissues and cells through application of TRIzol (Invitrogen, Carlsbad, CA, USA), followed by complementary DNA (cDNA) acquisition by a PrimeScript RT reagent Kit with gDNA Eraser (Takara, Dalian, China). qRT-PCR was performed with SYBR Green Master PCR mix (Applied Biosystems, Foster City, CA, USA) on the ABI 7900 system (Applied Biosystems). Expression of *HOXD-AS2*, *CCR1*, *DCP1A*, and *PPP3R1* or *miR-3681-5p*, calculated by $2^{-\Delta\Delta Ct}$ method was normalized to that of *GAPDH* or *U6*. Primers for this assay were as follows: *HOXD-AS2* forward 5'-AGGAACTGCTCTGGTGAACTCC-3' and reverse 5'-TGGGCATCTCTTTCAGGAAGGT-3'; *miR-3681-5p* forward 5'-TAGTGGATGATGCACTCTGT-3' and reverse 5'-GAACATGTCTGCGTATCTC-3'; *CCR1* forward 5'-GCCTTCTGGTTTTATGGG-3' and reverse 5'-CTCCTAGACACTTTTCCTC-3'; *DCP1A* forward 5'-CACCCCGGTGCTAATCACTC-3' and reverse 5'-GCTCAACGGGATTGTGTAGGTT-3'; *PPP3R1* forward 5'-GAGGGCGTCTCTCAGTTCAG-3' and reverse 5'-GCTGGACGTCTTGAGCAGAT-3'; *GAPDH* forward 5'-CGCTCTCTGCTCCTCCTGTTC-3' and reverse 5'-ATCCGTTGACTCCGACCTTCAC-3'; *U6* forward 5'-CTCGCTTCGGCAGCACA-3' and reverse 5'-ACGCTTCACGAATTTGCGT-3'.

Cell transfection

H1975 and A549 cells were cultured in the incubator at 37 ℃ in a humidified 5% CO_2 atmosphere for cell transfection. When cell confluency reached 60–80%, cells were subjected to transfection. All plasmids were from GenePharma (Shanghai, China). *HOXD-AS2* downregulation in tumor cells was achieved through treatment with small interfering RNAs (siRNAs) targeting *HOXD-AS2* (si-*HOXD-AS2*), in comparison with control and negative control (si-NC) groups. To explore the role of *HOXD-AS2 in vivo*, short hairpin RNAs (shRNAs) targeting *HOXD-AS2* (sh-*HOXD-AS2)* and sh-NC lentivirus (LV) were transfected into H1975 cells. Expression of *miR-3681-5p* was affected by transfection of *miR-3681-5p* mimic and anti-*miR-3681-5p*, compared with relative NCs. The sequence of *DCP1A* was amplified and cloned into a pcDNA3.1 vector to construct *DCP1A* overexpression vectors (oe-*DCP1A*), with blank vector as NC. This assay was conducted by Lipofectamine 2000 (Invitrogen) according to the manufacturer's protocols.

Bioinformatics analysis

A volcano plot was made according to Gene Expression Omnibus (GEO) database GSE138172 to identify differentially expressed genes (DEGs) in NSCLC and non-tumor tissues. Interaction between *HOXD-AS1* and *miR-3681-5p* was predicted through ENCORI (https://starbase.sysu.edu.cn/index.php). Predicted targets of *miR-3681-5p* by miRDB (https://mirdb.org/), TargetScan (https://www.targetscan.org/vert_80/), and DIANA (http://diana.imis.athena-innovation.gr/DianaTools/index.php) were analyzed to construct a Venn diagram on Venny 2.1.0 (https://bioinfogp.cnb.csic.es/tools/venny/index.html).

3-(4,5-dimethylthiazol-2-yl)-2,5-diphenyltetrazolium bromide (MTT) assay

MTT (Sigma Aldrich, St. Louis, MO, USA) was employed to test cell viability. Cells (4×10^3 in each well) were seeded into a 96-well culture dish 24 hours post transfection. After removal of the supernatant, 10 µL MTT was added to the well at 0, 24, 48, and 72 hours, followed by 4 hours of incubation. Dimethyl sulfoxide (DMSO) was added and shaken to sufficiently dissolve the purple crystals, and the optical density (OD) value was measured at 490 nm upon a microplate reader (Olympus, Tokyo, Japan).

Flow cytometry analysis

Cell apoptosis of tumor cells was assessed through flow cytometry with assistance of Annexin V-fluorescein isothiocyanate (FITC)/propidium iodide (PI) apoptosis kit (eBioscience; Thermo Fisher Scientific, Waltham, MA, USA) as per the guidance of producers. Collected cells from 6 well plates were centrifuged for 5 minutes and washed with phosphate-buffered saline (PBS), followed by incubation with 5 µL Annexin V-FITC and 5 µL PI for 15 minutes at room temperature. Thereafter, cells were dissected utilizing the BD FACScalibur flow cytometry [Becton, Dickinson, and Co. (BD) Biosciences, Franklin Lakes, NJ, USA].

Transwell experiments

Cell migration and invasion capabilities were explored via transwell experiments through usage of a transwell insert (8-µm pore size, Corning Costar, Corning, NY, USA) without or with Matrigel (Millipore, Bedford, MA, USA). For cell migration, serum-free DMEM was employed for obtaining cell suspension, which was thereafter put in the upper chamber. Medium with 10% FBS was put in the lower chamber. Cells were wiped from the lower surface of the upper chamber with a cotton swab and taken for fixation by 70% methanol and staining with 0.25% crystal violet for 20 minutes at room temperature. An optical microscope (Olympus, Tokyo, Japan) was applied to observe and count cells in 5 random fields. For cell invasion, the insert with Matrigel was employed.

Luciferase reporter assay

To assess the effect of *miR-3681-5p* on *HOXD-AS2*, H1975 and A549 cells were co-transfected with NC or *miR-3681-5p* mimic and the pmirGLO vector (Promega, Madison, WI, USA) with wild type (WT) or mutant type (MUT) sequences of *HOXD-AS2*. To assess the effect of *miR-3681-5p* on *DCP1A*, H1975 and A549 cells were co-transfected with NC or *miR-3681-5p* mimic and the pmirGLO vector with WT or MUT sequences of *DCP1A*. After 48 hours of transfection by Lipofectamine (Invitrogen, USA), luciferase activity was estimated utilizing the dual-luciferase reporter assay system (Promega, USA), with Renilla activity as normalization.

Xenograft tumor models

To interrogate the function of *HOXD-AS2* in NSCLC *in vivo*, animal models were established. A total of 10 4-week-old healthy male BALB/c nude mice (D000521) were obtained from Jiangsu Jicui Yaokang Biotechnology Co., Ltd. (GemPharmatech Co. Ltd., Nanjing, China) and kept in specific-pathogen-free conditions with free food and water. After subcutaneous injection of H1975 cells with LV-sh-NC or LV-sh-*HOXD-AS2* into the right flank, mice were randomly divided into sh-NC and sh-*HOXD-AS2* groups (n=5 in each group). Tumor growth was measured every 3 days using calipers, which was calculated as $V = 0.5 \times L \times W^2$ (L: length; W: width). Twenty-four days later, mice were euthanized through carbon dioxide (CO_2) inhalation and the tumors were removed for measuring weights and taking pictures. Experiments were performed in the laboratory animal center of Nanjing Agricultural University under a project license (No. 2022021) granted by the Ethics Committee of Nanjing Agricultural University, in compliance with institutional guidelines for the care and use of animals. A protocol was prepared before the study without registration.

Western blot

To examine protein expression, isolated specimens were lysed in radioimmunoprecipitation assay (RIPA) lysis buffer (Thermo Fisher Scientific, USA) and its concentration was estimated by bicinchoninic acid (BCA) kit (Thermo Fisher Scientific). A total of 20 µg of protein samples were thereafter isolated on 10% sodium dodecyl sulfate polyacrylamide gel electrophoresis (SDS-PAGE), followed by transferring onto polyvinylidene fluoride (PVDF) membranes (Millipore, Bedford, MA, USA). The membranes were subjected to blockade by 5% nonfat milk and cultivated overnight at 4 ℃. Primary antibodies against

DCP1A (22373-1-AP; 1:2,000; Proteintech, Rosemont, IL, USA) and *GAPDH* (ab8245; 1:500; Abcam, Cambridge, MA, USA) were employed. Thereafter, horseradish peroxidase (HRP)-tagged secondary antibody was applied to culture the membranes for another 1 hour. Blots were viewed with an enhanced chemiluminescence (ECL) kit (Pierce, Rockford, IL, USA), normalized to the internal reference GAPDH.

Hematoxylin and eosin (HE) staining

Obtained lung tissues were fixed by formalin, embedded in paraffin, and sectioned as 4 μm. Subsequently, sections were stained utilizing HE solution after deparaffinage. Histopathological characteristics were viewed using a light microscope (Leica Microsystems, Wetzlar, Germany).

Immunohistochemistry (IHC)

We soaked tissues in ethanol and rinsed them using PBS. Thereafter, samples were cultivated with a permeable solution with 3% H_2O_2 for another 10 minutes. We prepared 5% goat serum blocking solution for incubation for nearly 20 minutes. Antibody against Ki-67 (ab92742; 1:1,000; Abcam) was utilized for dilution and added to the sample at 4 ℃ overnight. After that, HRP-labelled anti-rabbit secondary antibody was applied for culture for 1 hour. Slides were developed with 3,3'-diaminobenzidine (DAB) and dyed utilizing hematoxylin, followed by observation under a microscope.

Statistical analysis

Data gained from triplicated tests were dissected with SPSS 20.0 (IBM Corp., Armonk, NY, USA) and presented as mean ± standard deviation (SD) with a 95% confidence interval (CI). A P value below 0.05 was considered statistically significant. Differences of two or multiple groups were compared using Student's *t*-test and one-way analysis of variance (ANOVA). Kaplan-Meier analysis was used to measure the correlation between *HOXD-AS2* expression and OS of cancer patients.

Results

HOXD-AS2 was upregulated in NSCLC and predicted poor prognosis

The GSE138172 dataset was analyzed via volcano plots to identify DEGs in NSCLC (*Figure 1A*). Among these genes, lncRNA *HOXD-AS2* is significantly overexpressed in NSCLC. Then, we tested its expression in 5 pairs of NSCLC and non-tumor tissues. The results of qRT-PCR demonstrated that *HOXD-AS2* exhibited obviously high expression in NSCLC tissues (*Figure 1B*). Kaplan-Meier analysis was performed for exploring the relation between *HOXD-AS2* expression and OS, which revealed that high *HOXD-AS2* expression predicted low OS rate (*Figure 1C*). The qRT-PCR assay indicated that *HOXD-AS2* expression was relatively heightened in NSCLC cells containing H1975, A549, and H1299, compared with normal pulmonary epithelial BEAS-2B cells (*Figure 1D*). The H1975 and A549 cells with higher expression of *HOXD-AS2* were chosen for subsequent assays. Here, it was clear that *HOXD-AS2* exhibited high expression in NSCLC tissues and cells and predicted worse prognosis.

HOXD-AS2 silencing impeded proliferation, migration, and invasion but induced apoptosis in NSCLC

To assess the function of *HOXD-AS2* in NSCLC, we applied si-HOXD-AS2 to downregulate *HOXD-AS2* expression. The results of qRT-PCR disclosed that in H1975 and A549 cells, *HOXD-AS2* expression was dramatically silenced by si-*HOXD-AS2* transfection (*Figure 2A*). Through MTT assay, we observed that downregulation of *HOXD-AS2* significantly repressed cell viability in comparison with control and si-NC groups (*Figure 2B*). The results of transwell assays presented that cell migration and invasion were distinctly inhibited when *HOXD-AS2* expression was downregulated (*Figure 2C*). Moreover, flow cytometry exhibited that cell apoptosis was overtly activated under transfection of si-*HOXD-AS2* in H1975 and A549 cells (*Figure 2D*). Taken together, inhibition of *HOXD-AS2* hindered proliferation, migration, and invasion but activated apoptosis in NSCLC cells.

HOXD-AS2 sponged miR-3681-5p to regulate cellular activities in NSCLC cells

To explore the molecular mechanism under *HOXD-AS2* in NSCLC, we browsed starBase and discovered the binding between *HOXD-AS2* and *miR-3681-5p*. The binding sequences were presented in *Figure 3A*. Then, luciferase reporter assay was utilized to affirm the interaction, in which an obvious decrease in luciferase activity of *HOXD-AS2*-WT was observed (*Figure 3B*). In NSCLC tissues,

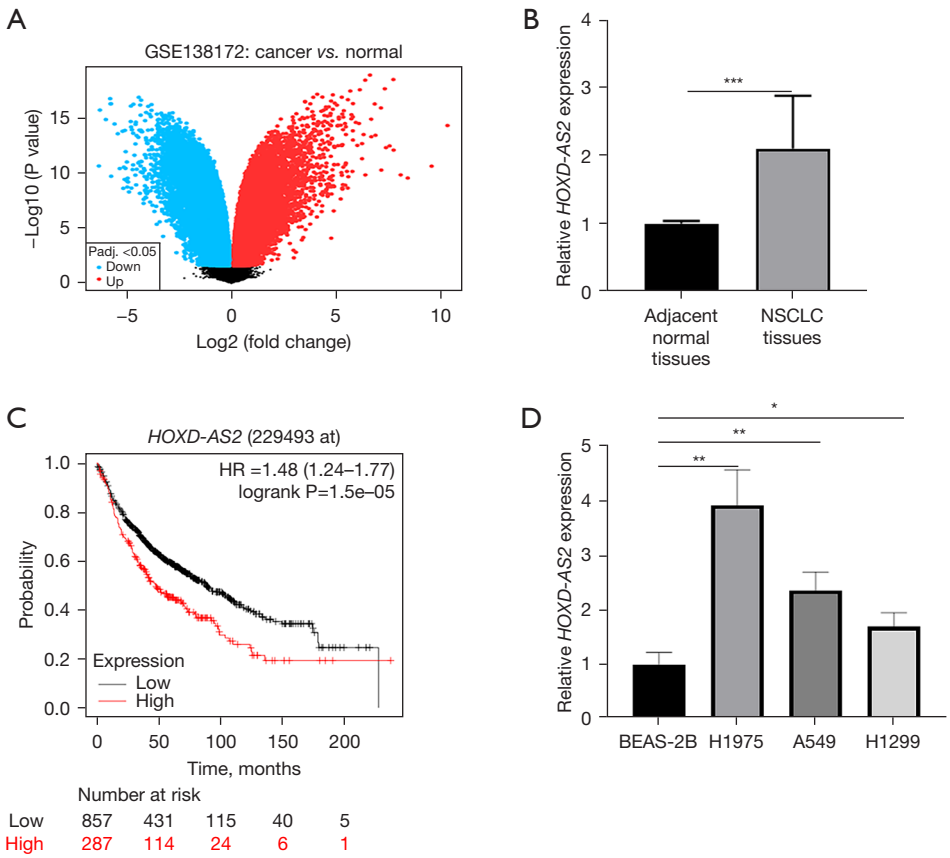

Figure 1 *HOXD-AS2* was upregulated in NSCLC and predicted poor prognosis. (A) Analysis of GSE138172 dataset by volcano plots for obtaining dysregulated genes in cancer and normal tissues. Black dots are genes with no significant expression changes in cancer and normal tissues. (B) qRT-PCR detection of *HOXD-AS2* expression in 5 paired NSCLC and adjacent normal tissues. (C) The relationship between *HOXD-AS2* expression and OS in NSCLC was explored through Kaplan-Meier analysis. (D) qRT-PCR assay was performed to test expression of *HOXD-AS2* in normal pulmonary epithelial cell line BEAS-2B and NSCLC cells (H1975, A549 and H1299). *, P<0.05; **, P<0.01; ***, P<0.001. HR, hazard ratio; NSCLC, non-small cell lung cancer; OS, overall survival; qRT-PCR, quantitative real-time polymerase chain reaction.

miR-3681-5p expression was distinctly decreased relative to normal tissues, as estimated by qRT-PCR (*Figure 3C*). Significantly low expression of *miR-3681-5p* was observed in H1975 and A549 cells, compared with BEAS-2B cells (*Figure 3D*). The qRT-PCR assay presented that *HOXD-AS2* silencing could upregulate *miR-3681-5p* expression, which was reduced under transfection of anti-*miR-3681-5p* (*Figure 3E*). The results of MTT assay demonstrated that cell viability was significantly repressed when *HOXD-AS2* was downregulated, which was strengthened when *miR-3681-5p* expression was inhibited (*Figure 3F*). Transwell experiments also represented that *HOXD-AS2* repression overtly hindered cell migration and invasion and the inhibition was restored when *miR-3681-5p* expression was reduced (*Figure 3G* and Figure S1A). In flow cytometry, *HOXD-AS2* decrease-activated cell apoptosis was distinctly restricted under *miR-3681-5p* reduction (*Figure 3H* and Figure S1B). In summary, *HOXD-AS2* sponged *miR-3681-5p* to mediate cellular activities in NSCLC cells.

MiR-3681-5p targeted DCP1A to boost NSCLC proliferation, migration, and invasion

A Venn diagram was drawn to identify the downstream targets of *miR-3681-5p*. Data from miRDB, TargetScan, and DIANA were analyzed and eventually, 3 targets including *CCR1*, *DCP1A*, and *PPP3R1* were screened (*Figure 4A*). After overexpression of *miR-3681-5p*, only *DCP1A*

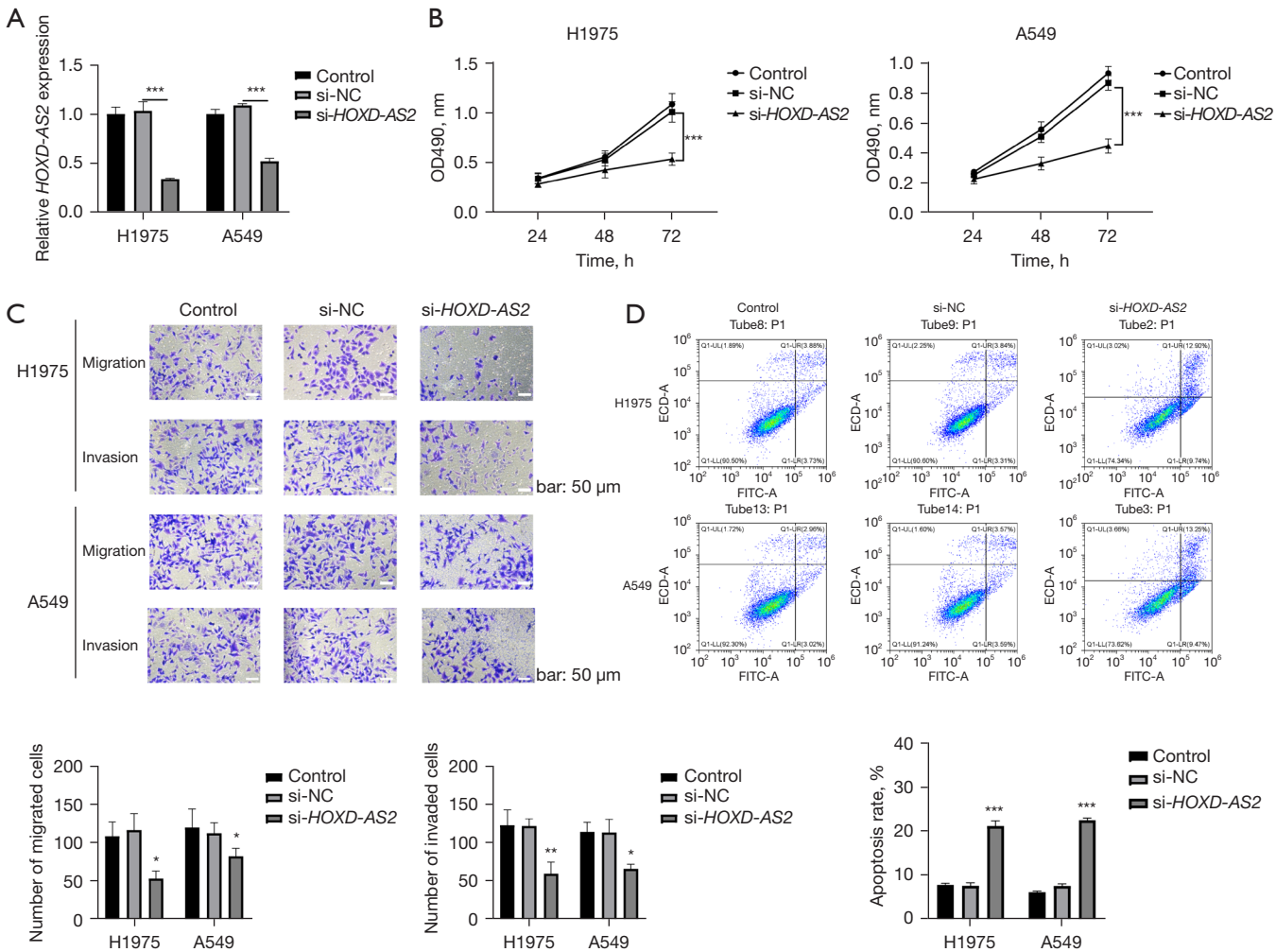

Figure 2 *HOXD-AS2* silencing impeded proliferation, migration, and invasion but induced apoptosis in NSCLC. (A) Control, si-NC, and si-*HOXD-AS2* were transfected into H1975 and A549 cells. qRT-PCR assay was applied to examine the transfection efficiency of si-*HOXD-AS2*. (B) The cell viability of H1975 and A549 cells was measured via MTT assay. (C) Cell migration and invasion abilities of H1975 and A549 cells were respectively detected under 3 treatments (crystal violet staining; scale bar: 50 μm), with quantification results exhibited in the pictures below. (D) Apoptosis of H1975 and A549 cells in the 3 groups was assessed by flow cytometry, with quantification results exhibited in the pictures below. *, P<0.05; **, P<0.01; ***, P<0.001. ECD, phycoerythrin-Texas Red; FITC, fluorescein isothiocyanate; NC, negative control; NSCLC, non-small cell lung cancer; qRT-PCR, quantitative real-time polymerase chain reaction; MTT, 3-(4,5-dimethylthiazol-2-yl)-2,5-diphenyltetrazolium bromide; OD, optical density; si, small interfering; UL, upper left; UR, upper right; LL, lower left; LR, lower right.

exhibited dramatically reduced expression in H1975 and A549 cells (*Figure 4B*). Thus, *DCP1A* was the predicted target of *miR-3681-5p* in NSCLC. The predicted binding sites between *miR-3681-5p* and *DCP1A* were shown in *Figure 4C*. Subsequent luciferase reporter experiments showed that *miR-3681-5p* bound to *DCP1A* (*Figure 4D*). Functional assays were also performed in H1975 and A549 cells to explore the function of *miR-3681-5p/DCP1A* axis in NSCLC. The transfection efficiency of oe-*DCP1A* was affirmed through qRT-PCR (*Figure 4E*). In the MTT assay, cell viability was significantly restricted by *miR-3681-5p* upregulation, which was partly recovered by increase of *DCP1A* (*Figure 4F*). Transwell experiments uncovered that *miR-3681-5p* elevation-restrained migration and invasion was rescued when *DCP1A* expression was obviously increased (*Figure 4G* and Figure S2A). Overexpression

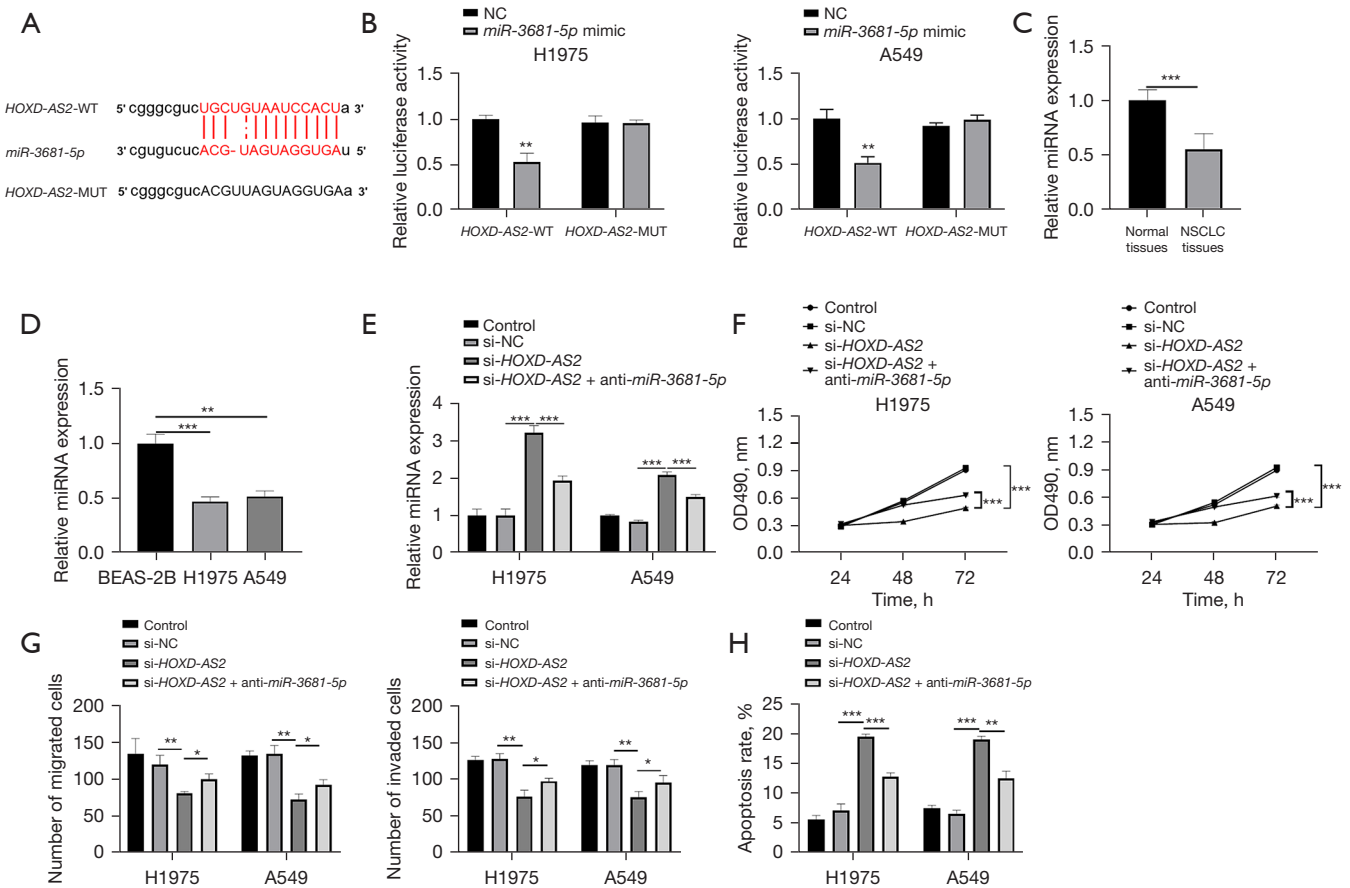

Figure 3 *HOXD-AS2* sponged *miR-3681-5p* in NSCLC cells. (A) Binding sequences of *HOXD-AS2* with *miR-3681-5p* were exhibited. (B) Luciferase reporter assay was conducted in H1975 and A549 cells to affirm the interaction between *HOXD-AS2* and *miR-3681-5p*. (C) *miR-3681-5p* expression in NSCLC and normal tissues was examined by qRT-PCR experiment. (D) qRT-PCR assay was used to test expression of *miR-3681-5p* in BEAS-2B, H1975, and A549 cells. (E) *MiR-3681-5p* expression in H1975 and A549 cells was evaluated by qRT-PCR. (F) The cell viability of the above 2 cells was tested via MTT assay. (G) Quantitative results of transwell assays to detect cell migration and invasion abilities of H1975 and A549 cells. (H) Quantitative results of flow cytometry to assess apoptosis of H1975 and A549 cells in 4 groups. *, P<0.05; **, P<0.01; ***, P<0.001. NC, negative control; NSCLC, non-small cell lung cancer; qRT-PCR, quantitative real-time polymerase chain reaction; MTT, 3-(4,5-dimethylthiazol-2-yl)-2,5-diphenyltetrazolium bromide; MUT, mutant; si, small interfering; WT, wild type; OD, optical density.

of *miR-3681-5p* obviously promoted apoptosis and the phenomenon was significantly suppressed with increase of *DCP1A* (*Figure 4H* and Figure S2B). Hence, *miR-3681-5p* targeted *DCP1A*, thus facilitating NSCLC proliferation, migration, and invasion.

Inhibition of HOXD-AS2 hampered NSCLC tumor growth in vivo

Animal models were established to investigate the role of *HOXD-AS2 in vivo*. H1975 cells subjected to lentiviral transfection with sh-NC or sh-*HOXD-AS2* were injected subcutaneously into nude mice. The recorded tumor volumes were displayed in *Figure 5A*, which indicated the inhibitory effect of *HOXD-AS2* silencing on tumor volume. Tumor weights and sizes were also decreased when *HOXD-AS2* was downregulated (*Figure 5B,5C*). We also used qRT-PCR and Western blot to test *miR-3681-5p* and *DCP1A* in tumor tissues and the results illustrated that *miR-3681-5p* was dramatically elevated and *DCP1A* protein expression was significantly decreased when *HOXD-AS2* was reduced (*Figure 5D,5E*). As exhibited in *Figure 5F*, HE staining

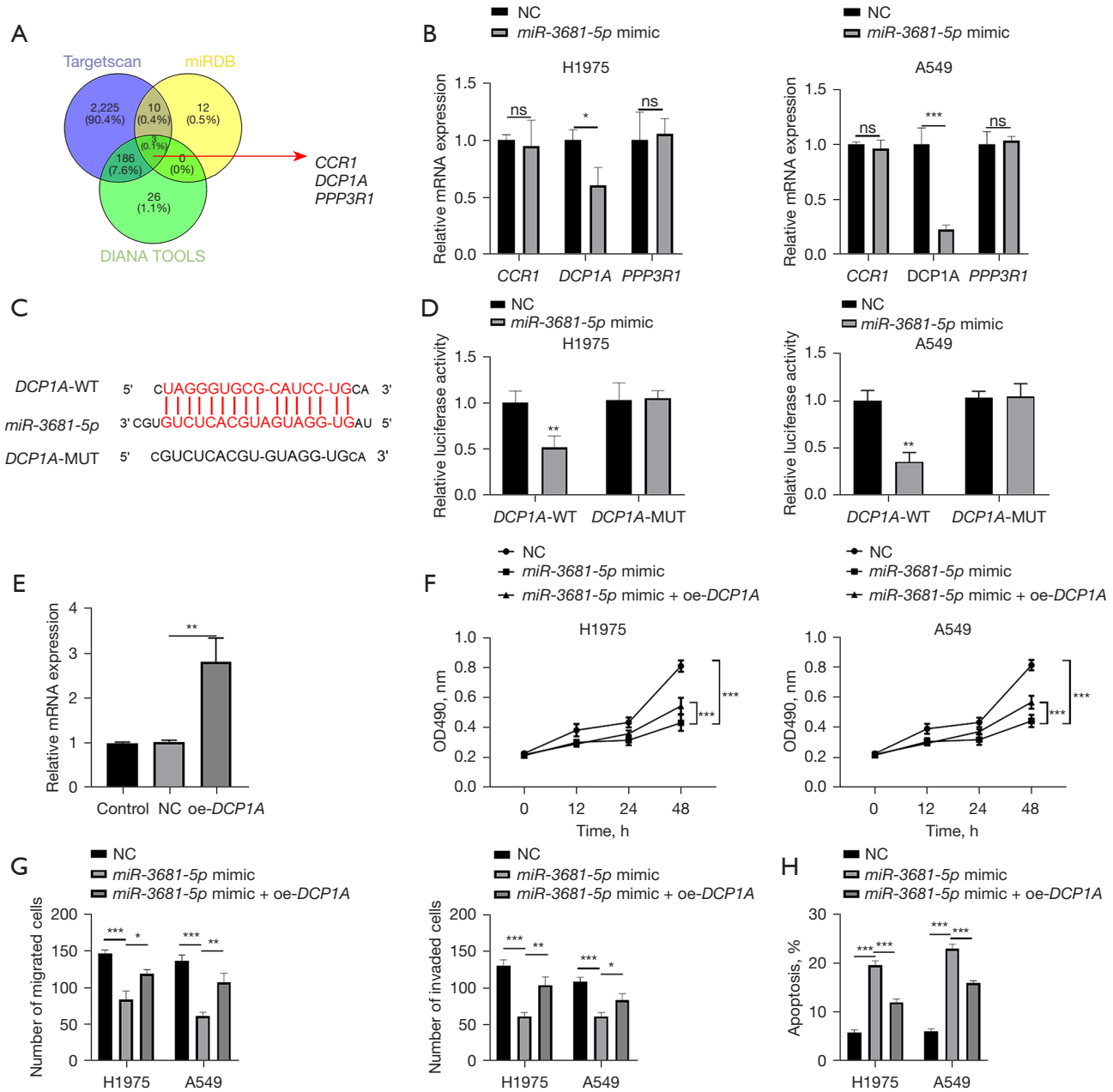

Figure 4 *MiR-3681-5p* targeted *DCP1A* to boost NSCLC proliferation, migration, and invasion. (A) Venn diagram of the shared targets of *miR-3681-5p* predicted by miRDB, TargetScan, and DIANA. (B) The mRNA expression of *CCR1*, *DCP1A*, and *PPP3R1* under *miR-3681-5p* overexpression was examined by qRT-PCR. (C) Binding sequences of *miR-3681-5p* with *DCP1A* were presented. (D) Tumor cells were transfected with NC and *miR-3681-5p* mimic respectively. The interaction between *miR-3681-5p* and *DCP1A* was validated through luciferase reporter assay. (E) qRT-PCR affirmed the transfection efficiency of oe-*DCP1A*. (F) MTT assay was employed to measure cell viability of H1975 and A549 cells treated with NC, *miR-3681-5p* mimic and *miR-3681-5p* mimic + oe-*DCP1A*. (G) Quantitative results of transwell assays to measure migration and invasion of H1975 and A549 cells under NC, *miR-3681-5p* mimic, and *miR-3681-5p* mimic + oe-*DCP1A* treatments. (H) Quantitative results of flow cytometry to test apoptosis of H1975 and A549 cells in 3 groups. *, P<0.05; **, P<0.01; ***, P<0.001. NC, negative control; NSCLC, non-small cell lung cancer; ns, not significant; qRT-PCR, quantitative real-time polymerase chain reaction; MTT, 3-(4,5-dimethylthiazol-2-yl)-2,5-diphenyltetrazolium bromide; MUT, mutant; WT, wild type; OD, optical density; oe, overexpression.

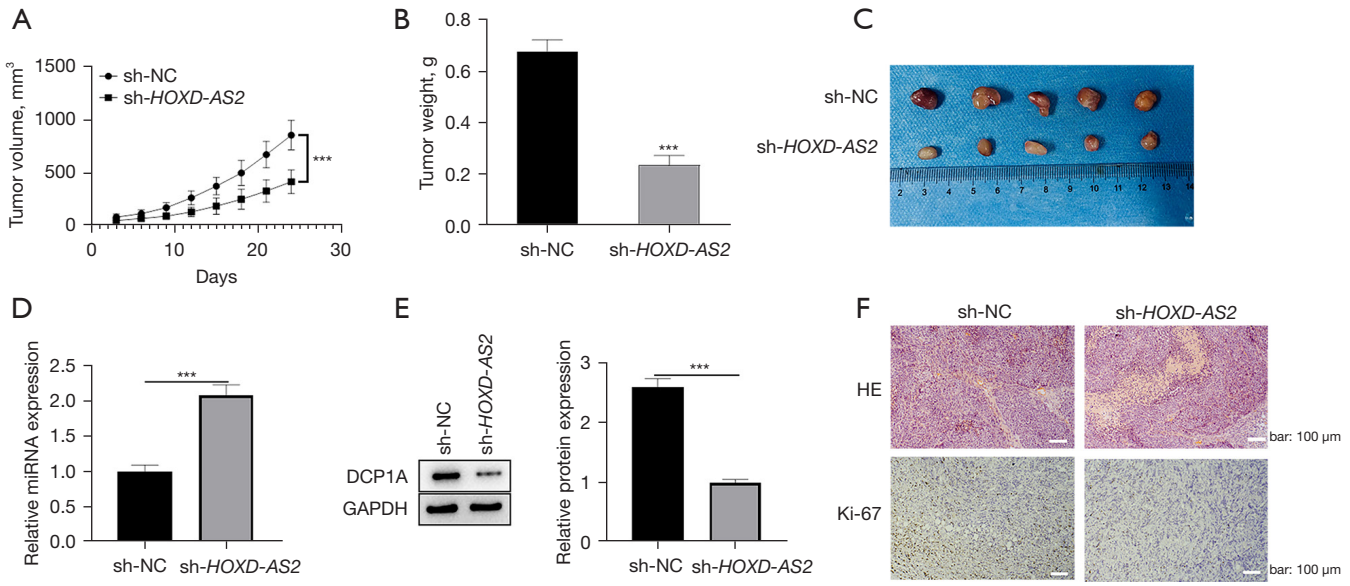

Figure 5 Inhibition of *HOXD-AS2* hampered NSCLC tumor growth *in vivo*. (A) H1975 cells transfected with LV-sh-NC and LV-sh-HOXD-AS2 were subcutaneously injected into nude mice. Tumor volumes were measured and analyzed. (B) Tumor weights were examined and recorded. (C) Pictures of tumors were presented. (D,E) *miR-3681-5p* and *DCP1A* expression in tumor tissues was assessed by qRT-PCR and Western blot. (F) HE staining of tumor tissues was performed; IHC was employed to analyze *Ki-67* expression (scale bar: 100 μm). ***, P<0.001. HE, hematoxylin and eosin; IHC, immunohistochemistry; LV, lentivirus; NC, negative control; sh, short hairpin; qRT-PCR, quantitative real-time polymerase chain reaction.

results indicated decreased tissue damage under *HOXD-AS2* downregulation. According to the results of IHC, *Ki-67* expression was obviously reduced with *HOXD-AS2* downregulation. Thus, *HOXD-AS2* silencing could inhibit NSCLC tumor growth *in vivo*.

Discussion

In ceRNA networks, lncRNAs competitively bind to miRNAs to cross-modulate each other, hence mediating downstream target genes of miRNAs at post-transcription level (27,28). In this regulatory mechanism, lncRNAs act as miRNA sponges via miRNA response elements (MREs) in the cytoplasm (29). Previously, lncRNAs-based ceRNA networks have been illustrated in different tumors. For examples, lncRNA DANCR accelerates proliferation and metastasis of pancreatic cancer cells via modulation of *miR-33b*/matrix metalloproteinase 16 (*MMP16*) expression (30); lncRNA *SNHG16* increases vascular endothelial growth factor (*VEGF*) levels in lung cancer upon its interaction with *miR-520*, and enhances the migration ability (31); in gallbladder cancer, *PVT1* mediates *HK2* expression via competitive binding with *miR-143* (32). In this paper, we observed the dramatically high expression of *HOXD-AS2* in NSCLC tissues compared with normal tissues based on GSE138172 results. In view of the tumor-promoting role of *HOXD-AS2* in glioma (15,33), we hypothesized that *HOXD-AS2* may also facilitate the progression of NSCLC. Hence, *HOXD-AS2* was chosen for research. Consistent with previous results, *HOXD-AS2* expression in NSCLC tissues and cells was relatively higher than that in normal tissues and cells. Moreover, NSCLC patients with high expression of *HOXD-AS2* exhibited short OS rate. Functional assays also affirmed that *HOXD-AS2* silencing significantly repressed cell viability, migration, invasion, and activated apoptosis of H1975 and A549 cells.

To clarify the molecular regulation mechanism of *HOXD-AS2* in NSCLC in detail, we browsed online and searched for the potential miRNAs binding with *HOXD-AS2*, among which *miR-3681-5p* attracted our attention. Previously, *miR-3681-5p* has only been demonstrated to interact with and be negatively mediated by *HOXD-AS2* to elevate *MALT1* expression in glioblastoma (16). Hence, we supposed that *miR-3681-5p* might involve in the regulation of *HOXD-AS2* on NSCLC. Our findings validated that *HOXD-AS2* bound with *miR-3681-5p*. The expression

of *miR-3681-5p* was distinctly downregulated in NSCLC tissues and cells, and was negatively related with *HOXD-AS2* level. The results of rescue assays unveiled that *miR-3681-5p* downregulation could abrogate the inhibitory effect of *HOXD-AS2* repression on cellular activities of H1975 and A549 cells. Herein, *miR-3681-5p* and its involvement in *HOXD-AS2* regulation were firstly explored in NSCLC.

Subsequently, we applied the TargetScan, miRDB, and DIANA websites to analyze the predicted targets of *miR-3681-5p*. The Venn diagram displayed 3 common targets, among which merely *DCP1A* exhibited an obvious decrease under *miR-3681-5p* overexpression. Ruan *et al.* has demonstrated that heightened *DCP1A* is associated with poor prognosis, and its downregulation decreases proliferation, migration, and chemotherapy resistance (24). In gastric cancer, *DCP1A* has been affirmed to be controlled by the *LINC00339/miR-377-3p* pathway and to accelerate tumor progression (26). In this study, *DCP1A* was affirmed to be targeted by *miR-3681-5p* and its overexpression could reverse the suppressed viability, migration, and invasion of NSCLC cells caused by *miR-3681-5p* promotion. The role of *DCP1A* and its related upstream mechanism in NSCLC was revealed for the first time.

In summary, these results indicated that *HOXD-AS2* exerts a promoting effect on proliferation, migration, and invasion through regulation of the *miR-3681-5p/DCP1A* axis in NSCLC, hinting the role of *HOXD-AS2* as an optional molecular target and diagnostic marker for further treatment and prognosis of NSCLC patients. However, the limitations of this study cannot be ignored. The diagnostic marker role of *HOXD-AS2* in NSCLC needs to be verified with more clinical samples. Functional experiments on other cellular activities were not performed. In future research, we will attempt to deeply study the potential relationships between *HOXD-AS2* and EMT, radioresistance, chemoresistance and ultimately recurrence, and its potential as a biomarker for patient risk stratification and local regional metastasis in NSCLC. For clinical studies, more NSCLC specimens and characteristics of NSCLC patients should be collected for analyzing the clinical application of lncRNA. For animal models, OS and the relationship with studied genes will also be explored.

Conclusions

HOXD-AS2 was upregulated in NSCLC tissues and cells, and its high expression predicted shorter OS rate. In NSCLC, *HOXD-AS2*, exerting its function via targeting *miR-3681-5p* to modulate *DCP1A*, could regulate the proliferation, migration, and invasion abilities of cells *in vitro* and *in vivo*.

Acknowledgments

Funding: None.

Footnote

Reporting Checklist: The authors have completed the ARRIVE and MDAR reporting checklists. Available at https://jtd.amegroups.com/article/view/10.21037/jtd-23-153/rc

Data Sharing Statement: Available at https://jtd.amegroups.com/article/view/10.21037/jtd-23-153/dss

Peer Review File: Available at https://jtd.amegroups.com/article/view/10.21037/jtd-23-153/prf

Conflicts of Interest: Both authors have completed the ICMJE uniform disclosure form (available at https://jtd.amegroups.com/article/view/10.21037/jtd-23-153/coif). The authors have no conflicts of interest to declare.

Ethical Statement: The authors are accountable for all aspects of the work in ensuring that questions related to the accuracy or integrity of any part of the work are appropriately investigated and resolved. Animal experiments were performed under a project license (No. 2022021) granted by the Ethics Committee of Nanjing Agricultural University, in compliance with institutional guidelines for the care and use of animals. Experiments involving human participants who provided signed informed consent before taking part were approved by the Ethics Committee of Binhai County People's Hospital (No. 2021BYKYLL006) and were conducted in accordance with the Declaration of Helsinki (as revised in 2013).

References

1. Baran K, Brzeziańska-Lasota E. Proteomic biomarkers of non-small cell lung cancer patients. Adv Respir Med 2021;89:419-26.
2. He T, Cao J, Xu J, et al. Minimally Invasive Therapies for Early Stage Non-small Cell Lung Cancer. Zhongguo Fei Ai Za Zhi 2020;23:479-86.
3. Smolle E, Leithner K, Olschewski H. Oncogene addiction and tumor mutational burden in non-small-cell lung cancer: Clinical significance and limitations. Thorac Cancer 2020;11:205-15.
4. Travis WD, Brambilla E, Nicholson AG, et al. The 2015 World Health Organization Classification of Lung Tumors: Impact of Genetic, Clinical and Radiologic Advances Since the 2004 Classification. J Thorac Oncol 2015;10:1243-60.
5. Alexander M, Kim SY, Cheng H. Update 2020: Management of Non-Small Cell Lung Cancer. Lung 2020;198:897-907.
6. Miller KD, Siegel RL, Lin CC, et al. Cancer treatment and survivorship statistics, 2016. CA Cancer J Clin 2016;66:271-89.
7. Anastasiadou E, Jacob LS, Slack FJ. Non-coding RNA networks in cancer. Nat Rev Cancer 2018;18:5-18.
8. Chan JJ, Tay Y. Noncoding RNA:RNA Regulatory Networks in Cancer. Int J Mol Sci 2018;19:1310.
9. Wilkes MC, Repellin CE, Sakamoto KM. Beyond mRNA: The role of non-coding RNAs in normal and aberrant hematopoiesis. Mol Genet Metab 2017;122:28-38.
10. Bhan A, Soleimani M, Mandal SS. Long Noncoding RNA and Cancer: A New Paradigm. Cancer Res 2017;77:3965-81.
11. Zhang W, Wang Q, Yang Y, et al. The role of exosomal lncRNAs in cancer biology and clinical management. Exp Mol Med 2021;53:1669-73.
12. Gupta S, Hashimoto RF. Dynamical Analysis of a Boolean Network Model of the Oncogene Role of lncRNA ANRIL and lncRNA UFC1 in Non-Small Cell Lung Cancer. Biomolecules 2022;12:420.
13. Wang D, Chen Y, Song X, et al. LncRNA OXCT1-AS1 promotes the proliferation of non-small cell lung cancer cells by targeting the miR-195/CCNE1 axis. Transl Cancer Res 2022;11:1255-68.
14. Liu SW, Yang P, Li FN, et al. LncRNA B4GALT1-AS1 promotes non-small cell lung cancer cell growth via increasing ZEB1 level by sponging miR-144-3p. Transl Cancer Res 2022;11:538-47.
15. Qin Y, Qi Y, Zhang X, et al. Production and Stabilization of Specific Upregulated Long Noncoding RNA HOXD-AS2 in Glioblastomas Are Mediated by TFE3 and miR-661, Respectively. Int J Mol Sci 2022;23:2828.
16. Zhong X, Cai Y. Long non-coding RNA (lncRNA) HOXD-AS2 promotes glioblastoma cell proliferation, migration and invasion by regulating the miR-3681-5p/MALT1 signaling pathway. Bioengineered 2021;12:9113-27.
17. Hussen BM, Hidayat HJ, Salihi A, et al. MicroRNA: A signature for cancer progression. Biomed Pharmacother 2021;138:111528.
18. Braicu C, Cojocneanu-Petric R, Chira S, et al. Clinical and pathological implications of miRNA in bladder cancer. Int J Nanomedicine 2015;10:791-800.
19. Li M, Li J, Ding X, et al. microRNA and cancer. AAPS J 2010;12:309-17.
20. Wang Z, Li TE, Chen M, et al. miR-106b-5p contributes to the lung metastasis of breast cancer via targeting CNN1 and regulating Rho/ROCK1 pathway. Aging (Albany NY) 2020;12:1867-87.
21. Wang Y, Hu J, Qi G, et al. miR-19a promotes the metastasis and EMT through CUL5 in prostate cancer cell line PC3. J BUON 2020;25:2028-35.
22. Zhao Y, Xu L, Wang X, et al. A novel prognostic mRNA/miRNA signature for esophageal cancer and its immune landscape in cancer progression. Mol Oncol 2021;15:1088-109.
23. Wang W, Lou W, Ding B, et al. A novel mRNA-miRNA-lncRNA competing endogenous RNA triple sub-network associated with prognosis of pancreatic cancer. Aging (Albany NY) 2019;11:2610-27.
24. Ruan T, Zhang Y, Liu W, et al. Expression of DCP1a in gastric cancer and its biological function and mechanism in chemotherapy resistance in gastric cancer cells. Dig Liver Dis 2020;52:1351-8.
25. Wu C, Liu W, Ruan T, et al. Overexpression of mRNA-decapping enzyme 1a affects survival rate in colorectal carcinoma. Oncol Lett 2018;16:1095-100.
26. Shi C, Liu T, Chi J, et al. LINC00339 promotes gastric cancer progression by elevating DCP1A expression via inhibiting miR-377-3p. J Cell Physiol 2019;234:23667-74.
27. Karreth FA, Pandolfi PP. ceRNA cross-talk in cancer: when ce-bling rivalries go awry. Cancer Discov 2013;3:1113-21.

28. Braga EA, Fridman MV, Moscovtsev AA, et al. LncRNAs in Ovarian Cancer Progression, Metastasis, and Main Pathways: ceRNA and Alternative Mechanisms. Int J Mol Sci 2020;21:8855.
29. Das S, Ghosal S, Sen R, et al. lnCeDB: database of human long noncoding RNA acting as competing endogenous RNA. PLoS One 2014;9:e98965.
30. Luo Y, Wang Q, Teng L, et al. LncRNA DANCR promotes proliferation and metastasis in pancreatic cancer by regulating miRNA-33b. FEBS Open Bio 2020;10:18-27.
31. Chen L, Qiu CH, Chen Y, et al. LncRNA SNHG16 drives proliferation, migration, and invasion of lung cancer cell through modulation of miR-520/VEGF axis. Eur Rev Med Pharmacol Sci 2020;24:9522-31.
32. Chen J, Yu Y, Li H, et al. Long non-coding RNA PVT1 promotes tumor progression by regulating the miR-143/HK2 axis in gallbladder cancer. Mol Cancer 2019;18:33.
33. Nie E, Jin X, Miao F, et al. TGF-β1 modulates temozolomide resistance in glioblastoma via altered microRNA processing and elevated MGMT. Neuro Oncol 2021;23:435-46.

(English Language Editor: J. Jones)

Cite this article as: Zhang Y, Ma H. LncRNA *HOXD-AS2* regulates *miR-3681-5p/DCP1A* axis to promote the progression of non-small cell lung cancer. J Thorac Dis 2023;15(3):1289-1301. doi: 10.21037/jtd-23-153

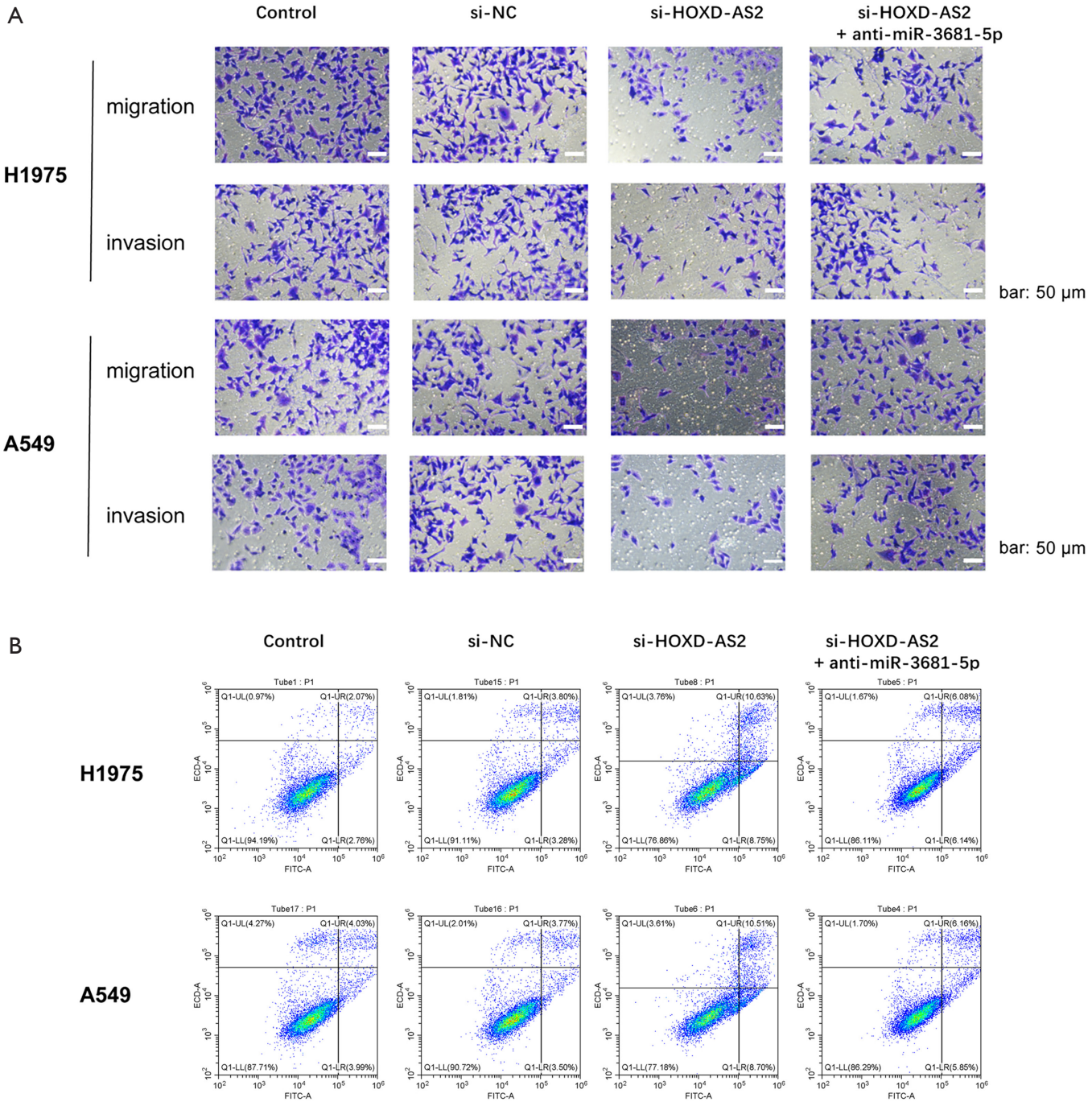

Figure S1 *HOXD-AS2/miR-3681-5p* axis modulated cell migration, invasion, and apoptosis. (A) Cell migration and invasion abilities of H1975 and A549 cells treated with Control, si-NC, si-*HOXD-AS2*, or si-*HOXD-AS2* + anti-*miR-3681-5p* were detected (crystal violet staining; scale bar: 50 μm). (B) Apoptosis of H1975 and A549 cells treated with Control, si-NC, si-*HOXD-AS2*, or si-*HOXD-AS2* + anti-*miR-3681-5p* in 4 groups was assessed by flow cytometry. ECD, phycoerythrin-Texas Red; FITC, fluorescein isothiocyanate; NC, negative control; UL, upper left; UR, upper right; LL, lower left; LR, lower right; si, small interfering.

https://dx.doi.org/10.21037/jtd-23-153

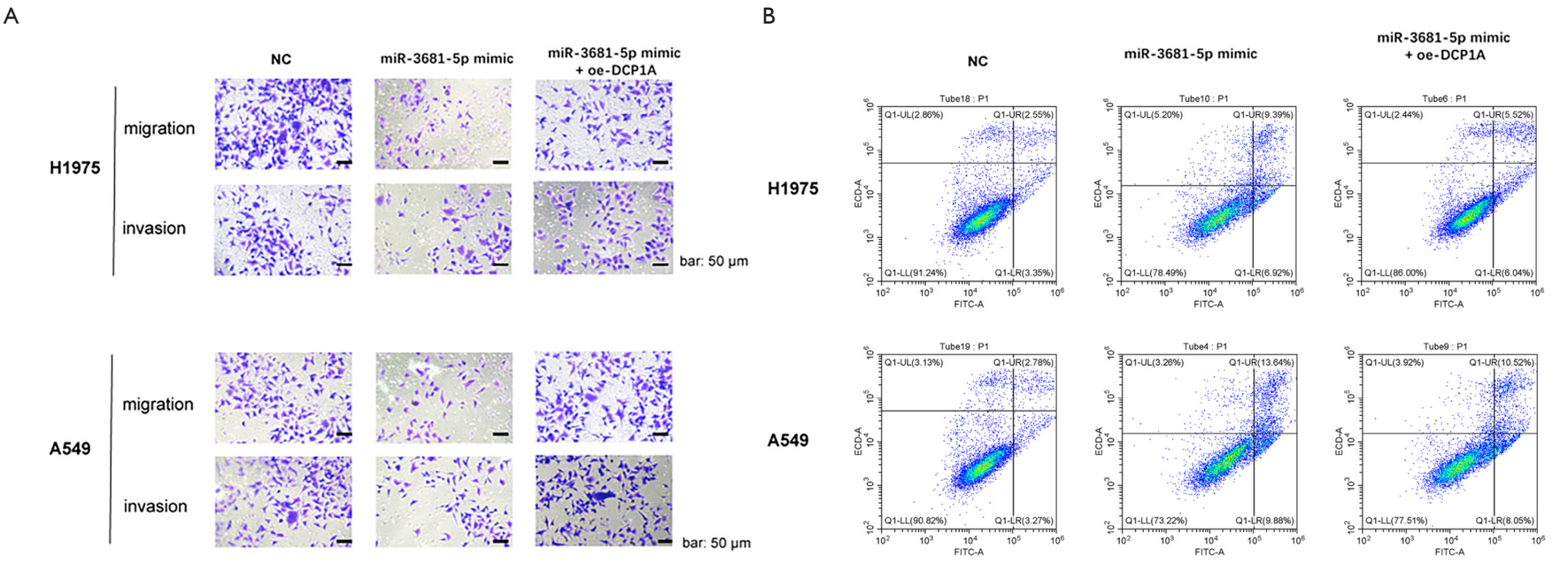

Figure S2 *MiR-3681-5p/DCP1A* axis modulated cell migration, invasion, and apoptosis. (A) Cell migration and invasion abilities of H1975 and A549 cells treated with NC, *miR-3681-5p* mimic, or *miR-3681-5p* mimic + oe-*DCP1A* were evaluated through transwell assays (crystal violet staining; scale bar: 50 μm). (B) Apoptosis of H1975 and A549 cells treated with NC, *miR-3681-5p* mimic, or *miR-3681-5p* mimic + oe-*DCP1A* were evaluated by flow cytometry. ECD, phycoerythrin-Texas Red; FITC, fluorescein isothiocyanate; NC, negative control; UL, upper left; UR, upper right; LL, lower left; LR, lower right; oe, overexpression.

https://dx.doi.org/10.21037/jtd-23-153